

Carbon sequestration potential of second-growth forest regeneration in the Latin American tropics

Robin L. Chazdon,^{1,2*} Eben N. Broadbent,³ Danaë M. A. Rozendaal,^{1,4,5} Frans Bongers,⁵ Angélica María Almeyda Zambrano,³ T. Mitchell Aide,⁶ Patricia Balvanera,⁷ Justin M. Becknell,⁸ Vanessa Boukili,¹ Pedro H. S. Brancalion,⁹ Dylan Craven,^{10,11,12} Jarcilene S. Almeida-Cortez,¹³ George A. L. Cabral,¹³ Ben de Jong,¹⁴ Julie S. Denslow,¹⁵ Daisy H. Dent,^{16,17} Saara J. DeWalt,¹⁸ Juan M. Dupuy,¹⁹ Sandra M. Durán,²⁰ Mario M. Espírito-Santo,²¹ María C. Fandino,²² Ricardo G. César,⁹ Jefferson S. Hall,¹⁰ José Luis Hernández-Stefanoni,¹⁹ Catarina C. Jakovac,^{5,23} André B. Junqueira,^{24,25,26} Deborah Kennard,²⁷ Susan G. Letcher,²⁸ Madelon Lohbeck,^{5,29} Miguel Martínez-Ramos,⁷ Paulo Massoca,²³ Jorge A. Meave,³⁰ Rita Mesquita,²³ Francisco Mora,^{7,30} Rodrigo Muñoz,³⁰ Robert Muscarella,^{31,32} Yule R. F. Nunes,²¹ Susana Ochoa-Gaona,¹⁴ Edith Orihuela-Belmonte,^{14†} Marielos Peña-Claros,⁵ Eduardo A. Pérez-García,³⁰ Daniel Piotta,³³ Jennifer S. Powers,³⁴ Jorge Rodríguez-Velázquez,⁷ Isabel Eunice Romero-Pérez,³⁰ Jorge Ruiz,^{35,36} Juan G. Saldarriaga,³⁷ Arturo Sanchez-Azofeifa,²⁰ Naomi B. Schwartz,³¹ Marc K. Steininger,³⁸ Nathan G. Swenson,³⁹ María Uriarte,³¹ Michiel van Breugel,^{10,40,41} Hans van der Wal,^{42,43} Maria D. M. Veloso,²¹ Hans Vester,⁴⁴ Ima Celia G. Vieira,⁴⁵ Tony Vizcarra Bentos,²³ G. Bruce Williamson,^{23,46} Lourens Poorter⁵

Regrowth of tropical secondary forests following complete or nearly complete removal of forest vegetation actively stores carbon in aboveground biomass, partially counterbalancing carbon emissions from deforestation, forest degradation, burning of fossil fuels, and other anthropogenic sources. We estimate the age and spatial extent of lowland second-growth forests in the Latin American tropics and model their potential aboveground carbon accumulation over four decades. Our model shows that, in 2008, second-growth forests (1 to 60 years old) covered 2.4 million km² of land (28.1% of the total study area). Over 40 years, these lands can potentially accumulate a total aboveground carbon stock of 8.48 Pg C (petagrams of carbon) in aboveground biomass via low-cost natural regeneration or assisted regeneration, corresponding to a total CO₂ sequestration of 31.09 Pg CO₂. This total is equivalent to carbon emissions from fossil fuel use and industrial processes in all of Latin America and the Caribbean from 1993 to 2014. Ten countries account for 95% of this carbon storage potential, led by Brazil, Colombia, Mexico, and Venezuela. We model future land-use scenarios to guide national carbon mitigation policies. Permitting natural regeneration on 40% of lowland pastures potentially stores an additional 2.0 Pg C over 40 years. Our study provides information and maps to guide national-level forest-based carbon mitigation plans on the basis of estimated rates of natural regeneration and pasture abandonment. Coupled with avoided deforestation and sustainable forest management, natural regeneration of second-growth forests provides a low-cost mechanism that yields a high carbon sequestration potential with multiple benefits for biodiversity and ecosystem services.

INTRODUCTION

Carbon emissions from tropical deforestation and degradation currently contribute an estimated 8 to 15% of annual global anthropogenic carbon emissions, further exacerbating global warming (1). National and global efforts to mitigate carbon emissions due to land-use change, such as the United Nations Reduced Emissions from Deforestation and Degradation program, focus primarily on reducing deforestation and degradation of intact tropical forests and enhancement of carbon stocks within disturbed forests, with less emphasis on reforestation and forest restoration (2, 3). Although deforestation in the world's tropical regions continues to reduce overall forest cover (4), second-growth forests (SFs) are expanding in many deforested areas of the Neotropics (5, 6). SFs emerge spontaneously in post-cultivation fallows, on abandoned farms and pastures, in the understory of ecological restoration plantings, and following assisted natural regeneration on private or communal lands (6, 7). Natural regeneration of forests is widely considered to be an effective low-cost mechanism for carbon sequestration, particularly in tropical regions (1, 2, 8, 9). Recent global estimates suggest that if tropical deforestation were halted entirely, if mature forests remain undisturbed, and if new forests were allowed to continue regrowing on deforested land, 24 to 35% of all carbon emissions from fossil fuels

and industrial production from 2000 to 2010 could be mitigated (10). Combined with reforesting unused agricultural land, these actions have been estimated to yield a global net carbon sequestration potential of 3 to 5 Pg C (petagrams of carbon) per year (1, 9).

Robust estimates of the carbon sequestration potential of naturally regrowing forests have been hampered by the lack of spatially explicit information on the extent and age distribution of SFs (including shifting cultivation fallows) and on the effects of climate and other environmental factors on local rates of biomass recovery. Assessments of carbon sequestration potential must account for effects of forest successional status, as well as effects of climate, land use, soils, and landscape context (6). Four key sources of uncertainty have impeded robust projections of the carbon sequestration potential of naturally regenerating tropical forests: (i) the age, longevity, and spatial distribution of regenerating forests and fallows; (ii) the potential for forest regeneration on previously forested land that is currently used for agriculture, pasture, or other nonforest land uses; (iii) the changes over time in aboveground carbon (AGC) storage in SFs under different environmental conditions (rainfall and soil fertility) and land-use history; and (iv) dynamics of agricultural land use and length of fallow cycles (11–13).

2016 © The Authors, some rights reserved; exclusive licensee American Association for the Advancement of Science. Distributed under a Creative Commons Attribution NonCommercial License 4.0 (CC BY-NC). 10.1126/sciadv.1501639

We reduce several of these uncertainties and estimate, for the first time, the carbon sequestration potential of SF regeneration over the entire Latin American tropical lowlands. We derive our projections using an extensive data set on biomass recovery during forest succession (14) and a map of estimated aboveground biomass (AGB) in 2008 derived from wall-to-wall remote sensing coverages (15). We estimate carbon sequestration potential under different scenarios of forest regeneration and pasture abandonment. These projections can help guide national policies to mitigate carbon emissions through nature-based approaches, including passive and active restoration approaches, intensification of pasture stocking rates (16), payment for environmental services programs, offsets as components of active restoration planning, or legal compliance with forest legislation (17). Our study addresses four main questions: (i) What is the area and estimated age distribution of SFs in the lowland Neotropics? (ii) What is the total predicted carbon storage potential of naturally regenerating forests over four decades across biomes and countries? (iii) How much carbon is sequestered under different scenarios of natural regeneration of pastures and persistence of SFs? (iv) How does the carbon sequestration potential of SF regeneration vary across countries?

To determine the carbon sequestration potential of regenerating forests, we first modeled the area and age distribution of existing SFs up to 100 years old. We used a 2008 map of Neotropical AGB in woody vegetation (15) to infer stand age using an equation relating biomass to climate and forest age on the basis of 43 successional chronosequences and 1148 plots across the lowland Neotropics (14). This map provides the most accurate spatially explicit data on forest biomass currently available and is based on a large network of field plots coupled with satellite LiDAR (light detection and ranging) to parameterize MODIS (Moderate Resolution Imaging Spectroradiometer) satellite data at a spatial resolution of 500 m (15). Additionally, we incorporated data on the spatial extent of croplands and pastures across Latin America

on the basis of the most recent coverages available at this geographic scale. We then projected future AGB accumulation of SFs (≤ 60 years) from 2008 to 2048. Our projections account for regional variation in climatic water availability, which strongly influences rates of biomass recovery across our study area (14).

Our projections do not assume any tree planting or assisted regeneration practices beyond creating conditions that permit natural regeneration, such as fencing or fire protection. To account for natural or assisted regeneration on former pastures and the potential re-clearing of SFs, we model carbon storage scenarios where only 80, 60, 40, 20, and 0% of young SFs (YSFs; 1 to 20 years) and mid-SFs (MSFs; 20 to 60 years) and 0 to 40% of pasture areas are permitted to regenerate naturally. Randomly selected second-growth areas are prevented from natural regeneration, and existing carbon stocks in these pixels are reduced to the mean level of agricultural lands in our 2008 baseline to simulate forest conversion to agriculture. We do not model any changes in extent of existing croplands, as we only consider changes in carbon storage resulting from regeneration of existing SFs or pasture areas.

RESULTS

Estimated areas of forest and farmland and initial carbon stocks

Our analysis showed that, in 2008, 20.1% of the 8.7 million km² of forest and farmland in our study area (1.75 million km²) was farmland, dominated by 1.2 million km² of pasture. Modeled areas of YSFs and MSFs (≤ 60 years) composed 28.1% (2.4 million km²) of the study area, whereas old SFs (60 to 100 years) composed 5.3% (461,519 km²). Only 46.5% of the study area (4.0 million km²) consisted of old-growth forest (OGF, arbitrarily defined as >100 years; Fig. 1A and Table 1). Modeled areas of YSFs and MSFs were distributed across all biomes and countries

¹Department of Ecology and Evolutionary Biology, University of Connecticut, Storrs, CT 06269–3043, USA. ²International Institute for Sustainability, Estrada Dona Castorina 124, Rio de Janeiro, CEP 22460-320, Brazil. ³Spatial Ecology and Conservation Lab, Department of Geography, University of Alabama, Tuscaloosa, AL 35487, USA. ⁴Department of Biology, University of Regina, 3737 Wascana Parkway, Regina, Saskatchewan S4S 0A2, Canada. ⁵Forest Ecology and Forest Management Group, Wageningen University, P.O. Box 47, 6700 AA Wageningen, Netherlands. ⁶Department of Biology, University of Puerto Rico, P.O. Box 23360, San Juan, PR 00931-3360, Puerto Rico. ⁷Instituto de Investigaciones en Ecosistemas y Sustentabilidad, Universidad Nacional Autónoma de México, CP 58089, Morelia, Michoacán, México. ⁸Department of Ecology and Evolutionary Biology, Brown University, Providence, RI 02912, USA. ⁹Department of Forest Sciences, "Luiz de Queiroz" College of Agriculture, University of São Paulo, Av. Pádua Dias, 11, 13418-900 Piracicaba, São Paulo, Brazil. ¹⁰SI ForestGEO, Smithsonian Tropical Research Institute, Roosevelt Avenue, 401 Balboa, Ancon, Panama. ¹¹German Centre for Integrative Biodiversity Research (iDiv) Halle-Jena-Leipzig, Deutscher Platz 5e, 04103 Leipzig, Germany. ¹²Institute for Biology, Leipzig University, Johannisallee 21, 04103 Leipzig, Germany. ¹³Departamento de Botânica-CCB, Universidade Federal de Pernambuco, Pernambuco, CEP 50670-901, Brazil. ¹⁴Department of Sustainability Science, El Colegio de la Frontera Sur, Av. Rancho Polígono 2-A, Ciudad Industrial, Lerma 24500, Campeche, Mexico. ¹⁵Department of Ecology and Evolutionary Biology, Tulane University, New Orleans, LA 70118, USA. ¹⁶Smithsonian Tropical Research Institute, Roosevelt Avenue, 401 Balboa, Ancon, Panama. ¹⁷Biological and Environmental Sciences, University of Stirling, Stirling FK9 4LA, UK. ¹⁸Department of Biological Sciences, Clemson University, 132 Long Hall, Clemson, SC 29634, USA. ¹⁹Centro de Investigación Científica de Yucatán A.C. Unidad de Recursos Naturales, Calle 43 # 130, Colonia Chuburná de Hidalgo, C.P. 97200, Mérida, Yucatán, México. ²⁰Earth and Atmospheric Sciences Department, University of Alberta, Edmonton, Alberta T6G 2EG, Canada. ²¹Departamento de Biología Geral, Universidade Estadual de Montes Claros, Montes Claros, Minas Gerais, CEP 39401-089, Brazil. ²²Fondo Patrimonio Natural para la Biodiversidad y Areas Protegidas, Calle 72 No. 12-65 piso 6, 110231 Bogota, Colombia. ²³Biological Dynamics of Forest Fragments Project, Environmental Dynamics Research Coordination, Instituto Nacional de Pesquisas da Amazonia, Manaus, Amazonas, CEP 69067-375, Brazil. ²⁴Centre for Crop Systems Analysis, Wageningen University, P.O. Box 430, 6700 AK Wageningen, Netherlands. ²⁵Knowledge, Technology and Innovation Group, Wageningen University, P.O. Box 8130, 6700 EW Wageningen, Netherlands. ²⁶Coordenação de Tecnologia e Inovação, Instituto Nacional de Pesquisas da Amazonia, Av. André Araújo 2936, Aleixo, 69060-001 Manaus, Brazil. ²⁷Department of Physical and Environmental Sciences, Colorado Mesa University, 1100 North Avenue, Grand Junction, CO 81501, USA. ²⁸Department of Environmental Studies, Purchase College (SUNY), 735 Anderson Hill Road, Purchase, NY 10577, USA. ²⁹World Agroforestry Centre (ICRAF), P.O. Box 30677-00100, Nairobi, Kenya. ³⁰Departamento de Ecología y Recursos Naturales, Facultad de Ciencias, Universidad Nacional Autónoma de México, Mexico City, C.P. 04510, México. ³¹Department of Ecology, Evolution and Environmental Biology, Columbia University, New York, NY 10027, USA. ³²Section of Ecoinformatics and Biodiversity, Department of Bioscience, Aarhus University, Aarhus 8000, Denmark. ³³Centro de Formação em Ciências Agroflorestais, Universidade Federal do Sul da Bahia, Itabuna-BA, 45613-204, Brazil. ³⁴Departments of Ecology, Evolution, and Behavior and Plant Biology, University of Minnesota, Saint Paul, MN 55108, USA. ³⁵School of Social Sciences, Geography Area, Universidad Pedagógica y Tecnológica de Colombia, 150003 Tunja, Colombia. ³⁶Department of Geography, 4841 Ellison Hall, University of California, Santa Barbara, Santa Barbara, CA 93106, USA. ³⁷Cr 5 No 14-05, P.O. Box 412, Cota, Cundinamarca, Colombia. ³⁸Department of Geographical Sciences, University of Maryland, College Park, MD 20742, USA. ³⁹Department of Biology, University of Maryland, College Park, MD 20742, USA. ⁴⁰Yale-NUS College, 12 College Avenue West, Singapore 138610, Singapore. ⁴¹Department of Biological Sciences, National University of Singapore, 14 Science Drive 4, Singapore 117543, Singapore. ⁴²Departamento de Agricultura, Sociedad y Ambiente, El Colegio de la Frontera Sur, Unidad Villahermosa, 86280 Centro, Tabasco, México. ⁴³Institute for Biodiversity and Ecosystem Dynamics, University of Amsterdam, 1090 Amsterdam, Netherlands. ⁴⁴Bonhoeffer College, Bruggertstraat 60, 7545 AX Enschede, Netherlands. ⁴⁵Museu Paraense Emilio Goeldi, C.P. 399, CEP 66040-170, Belém, Pará, Brazil. ⁴⁶Department of Biological Sciences, Louisiana State University, Baton Rouge, LA 70803–1705, USA.

*Corresponding author. Email: robin.chazdon@uconn.edu

†Present address: National Institute of Ecology and Climate Change, Periférico 5000, Col. Insurgentes Cuicuilco, Delegación Coyoacán, C.P. 04530, México.

but were most extensive (2.2 million km²) in six countries: Brazil, Mexico, Colombia, Venezuela, Bolivia, and Peru (Fig. 2A and table S2). In 2008, the entire study region was estimated to have a total aboveground C stock of 85.1 Pg. Farmland accounted for 10.2% of the total 2008 C stock (8.7 Pg), with 6.2 Pg C in pastures (Table 1). YSFs and MSFs accounted for 18.3% (15.6 Pg C) of this total, old SFs accounted for 6.4% (5.4 Pg C), and OGFs accounted for 65.1% (55.4 Pg C; Fig. 1B and Table 1).

Carbon sequestration scenarios

In Fig. 2B, we map the carbon sequestration scenario where 100% of YSFs (1 to 20 years) and MSFs (20 to 60 years) in the 2008 baseline

map are allowed to regenerate for 40 years at rates predicted by post-abandonment chronosequence studies (14). These age classes rapidly accumulate biomass and are the most prevalent across the study region. Under the 100% regeneration assumption, AGC stock increased 2.0-fold in YSFs and 1.2-fold in MSFs, yielding a potential total carbon sequestration of 8.48 Pg C over 40 years (Fig. 1C and Table 1), corresponding to a total sequestration of 31.09 Pg CO₂. This total is equivalent to carbon emissions from fossil fuel use and industrial processes in all of Latin America and the Caribbean from 1993 to 2014 (18).

Uncertainty estimates for total potential AGC sequestration in YSFs and MSFs from 2008 to 2048 range from 6.7 to 10.9 Pg C. Neotropical countries vary markedly in carbon sequestration potential (Fig. 1E) as a

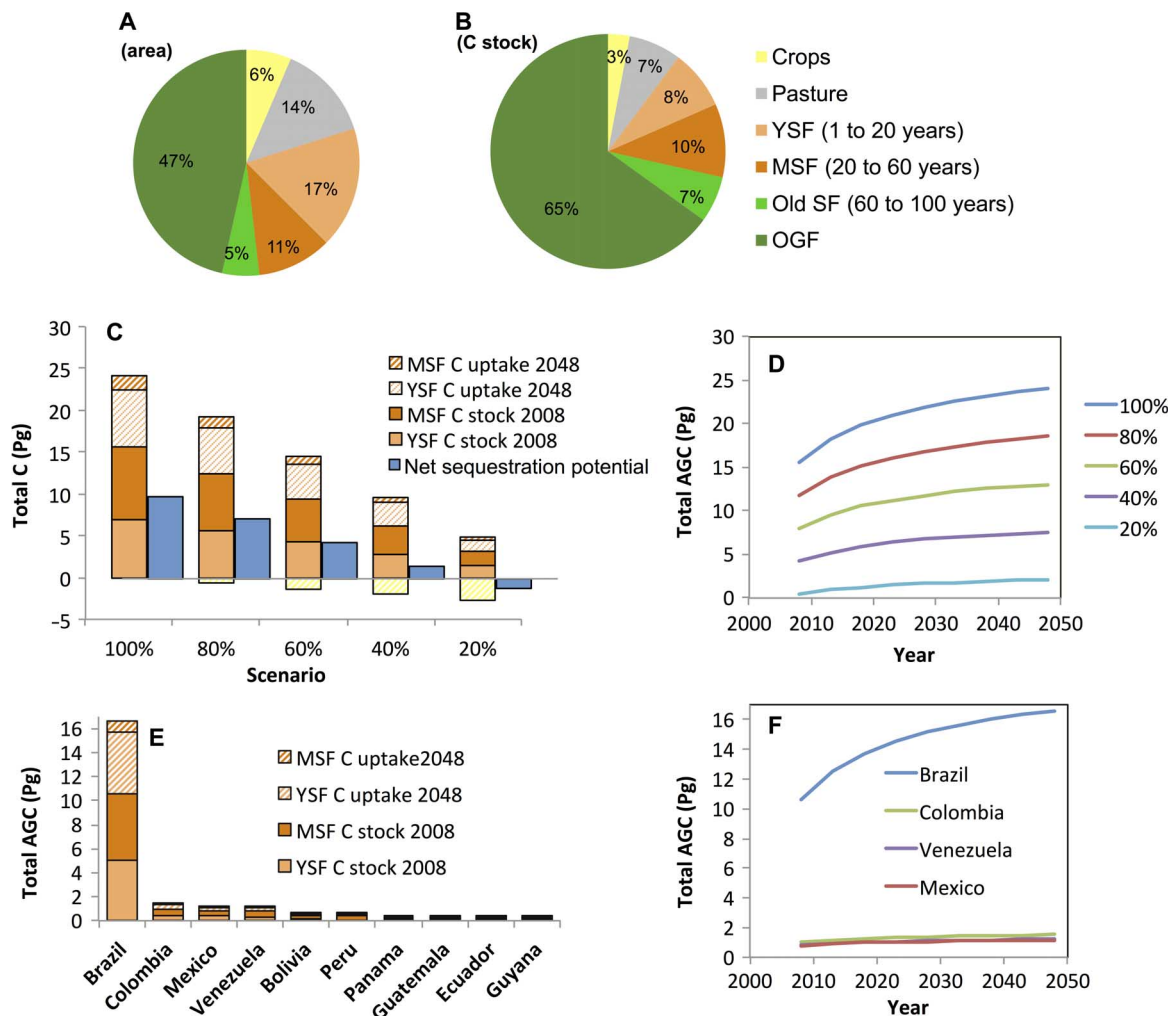


Fig. 1. Area and carbon distributions in SFs in the lowland Neotropics. (A and B) Percentages of modeled forest area (A) and AGC stock (B) in different land cover and forest age classes in 2008: cropland, pasture, forest <20 years (YSF), forest 20 to 60 years (MSF), forest 60 to 100 years (old SF), and forest >100 years (arbitrarily used as cutoff for OGF). (C) AGC stocks of YSFs and MSFs in 2008 (filled bars), and their net carbon sequestration from 2008 to 2048 (hatched bars). The total size of the bar indicates the total carbon stocks of those forests in 2048. Stacked bars are shown for five scenarios, where 100, 80, 60, 40, and 20% of the area are allowed to recover. The hatched yellow bar below the zero line indicates the carbon loss under these scenarios due to forest conversion to pasture or cropland in 2008, and the blue bar indicates the net sequestration potential of the different scenarios (carbon sequestration from 2008 to 2048 minus conversion-driven carbon loss in 2008). (D) Total AGC of YSFs and MSFs over the period 2008–2048 under different regeneration scenarios. (E) AGC of YSFs and MSFs in 2008, and their net carbon sequestration from 2008 to 2048 given 100% recovery, for each country separately. The total size of the bar indicates the total carbon stocks (AGC) of those forests in 2048. (F) Total AGC of YSFs and MSFs from 2008 to 2048 for the four countries with the largest carbon sequestration potential in naturally regenerating forests (see table S2 for more details).

result of differences in the extent and geographical distribution of SFs in wet and dry forest biomes (table S2). Brazil, by far, has the highest carbon storage potential in YSFs and MSFs (6.04 Pg C; 71.3%), followed by Colombia, Mexico, and Venezuela (Fig. 1, E and F). Ten countries accounted for 95.1% of the potential net carbon sequestration in YSFs and MSFs from 2008 to 2048 (Fig. 1E). National differences in potential sequestration increase over time (Fig. 1F). Mean annual rates of carbon storage of YSFs and MSFs were greatest from 2008 to 2013, when they potentially stored an average of 0.526 Pg C per year. These rates declined in 2043–2048, where they sequestered an average of 0.081 Pg C per year. Within only the first 5 years, the potential AGC stored from regeneration of YSFs and MSFs (100% scenario; 2.6 Pg C) can mitigate 9.64 Pg CO₂ emissions, which is more than the total CO₂ emissions from fossil fuel consumption and industrial processes from all countries in Latin America and the Caribbean from 2010 to 2014 (8.67 Pg) (18).

When less SF area is allowed to persist, the net carbon storage in YSFs and MSFs declines proportionately from 8.48 Pg C (100% recovery) to -1.16 Pg C (Fig. 1C). In the scenario where only 20% of the SF is allowed to persist and regenerate, carbon gains are lower than carbon losses because of forest clearing for agriculture, resulting in a net negative carbon sequestration outcome (Fig. 1C). When 40% of pastures are allowed to regenerate, an additional 2.0 Pg C can be sequestered, regardless of the level of SF persistence (Fig. 3). Similar levels of carbon storage can be achieved through different combinations of SF conservation and forest regeneration following pasture abandonment.

DISCUSSION

Natural regeneration provides a low-cost, nature-based solution for carbon sequestration with enormous potential in the Neotropics. This potential has been overlooked by the 2014 Intergovernmental Panel on Climate Change report, which suggests that the most cost-effective sequestration options in forestry are reducing deforestation, sustainable forest management, and afforestation (19). These findings have major implications for policies affecting forest land use, legal instruments, and

Table 1. Area and AGC stocks in 2008, and mean values of projected AGC sequestration over 40 years for six land cover types: YSF (≤20 years), MSF (20 to 60 years), old SF (60 to 100 years), OGF (>100 years, arbitrarily set), pasture, and crops. Carbon gains for old SF and OGF are not shown, because they cannot be estimated accurately. Values of net carbon assume zero deforestation of SFs.

Land use	2008		Net C gain (2008–2048)
	Area (km ²)	AGC (Pg)	AGC (Pg)
YSF	1,512,668	6.9796	6.8402
MSF	925,936	8.6028	1.6366
Old SF	461,518	5.4407	—
OGF	4,043,058	55.3859	—
Pasture	1,186,260	6.1718	4.9925
Crops	558,306	2.5356	2.6330
Total	8,687,747	85.1163	16.1023

economic incentives for SF regeneration, restoration, and conservation in Latin America (20). Combined with halting new deforestation and sustainably managing tropical forests, the significant carbon sequestration potential delivered by SFs provides essential solutions for reaching national and international carbon mitigation targets and supports ambitious forest restoration goals motivated by the Convention on Biological Diversity Aichi Targets (2010), the Bonn Challenge (2011), and the New York Declaration on Forests (2014), which calls for ending natural forest loss and restoring 350 million ha of forest worldwide by 2030.

Our model of SF age and geographic distribution within the lowland Latin American tropics yields 28% of total forest and agricultural area in YSFs and MSFs in 2008. This percentage is higher than the estimate of 23% by the United Nations Food and Agriculture Organization, which is not derived from mapping or modeling based on remote sensing-based products (21). This discrepancy highlights the challenges in estimating the cover of tropical SFs (6). Techniques for mapping the age and extent of SFs at pixel sizes below 25 ha are urgently needed to provide more spatially accurate assessments of SF extent and carbon sequestration potential at the country and regional levels (22, 23). Landsat-based coverages of land-use change can potentially provide such information, provided that SFs are distinguished from tree and oil palm plantations (7, 24). As forest patches are often considerably smaller than 25 ha, one limitation of our study is that mean pixel age may reflect the mixture of different forest ages and land cover types within each pixel. This spatial mixing may result in overrepresentation of mid-age values and an overestimation of the areal extent of secondary forests.

The carbon sequestration potential revealed by our study is likely an underestimate of the actual potential, for several reasons. Belowground carbon stocks in soils and roots will add 25% or more to total carbon storage (25), but knowledge regarding determinants of successional dynamics of belowground carbon sequestration is insufficient to include in our projections (26). Our study area excludes montane areas of Latin America, where SF is regenerating spontaneously on abandoned farmland (5). Our estimates could be further improved using higher-resolution spatial data, which are rapidly becoming available (27), explicitly taking local landscape matrix conditions into account (6), accounting for belowground carbon dynamics (28), and incorporating effects of previous land use on biomass recovery (28, 29). Future projections using more recent baseline data will rely on newer spatial analyses of forest biomass and agricultural land use across Latin America when these become available. Similarly, forest regrowth in the African and Asian tropics offers substantial carbon sequestration opportunities that are not included in our study (30–32). Our projections of carbon sequestration during forest succession, however, do not consider potential negative effects of climate change and extended droughts on rates of biomass accumulation (33).

Protecting SFs from deforestation poses many challenges, including the lack of legal definitions for SF (or lack of enforcement of existing definitions) and the absence of effective policy instruments and economic incentives for landowners (20). Currently, SFs are highly dynamic within Neotropical lowlands; the estimated time for half of the secondary forest to be removed within a 25 km × 25 km cell in the Brazilian Amazon averaged 5.4 years (12). Scenarios of carbon sequestration based on varying rates of forest and pasture regeneration can inform national-level commitments to restore forests through both active and passive pathways. Maps of potential carbon sequestration (Fig. 2B and figs. S1 to S3) provide spatially explicit guidance and realistic expectations for Latin American countries that are developing their

Intended Nationally Determined Contributions (INDCs) as part of their United Nations Framework Convention on Climate Change agreements. For example, Brazil's INDC aims to restore and reforest 12 million ha of Atlantic Forest by 2030 and restore an additional 15 million ha of degraded pasturelands by 2030 (34).

Governments, multinational organizations, nongovernmental organizations, and local stakeholders can leverage this climate change mitigation potential by enabling spontaneous or assisted natural regen-

eration in areas with suitable ecological conditions, by providing incentives to enhance agricultural productivity on degraded lands, and by avoiding further clearance of young and old forests. Our map indicates regions that are optimal for long-term carbon storage because of the natural regeneration of forests, presenting low-cost and high-yield carbon mitigation solutions. Carbon sequestration can be achieved through protection and enhancement of young second-growth areas and agricultural intensification on some parts of the land, judiciously

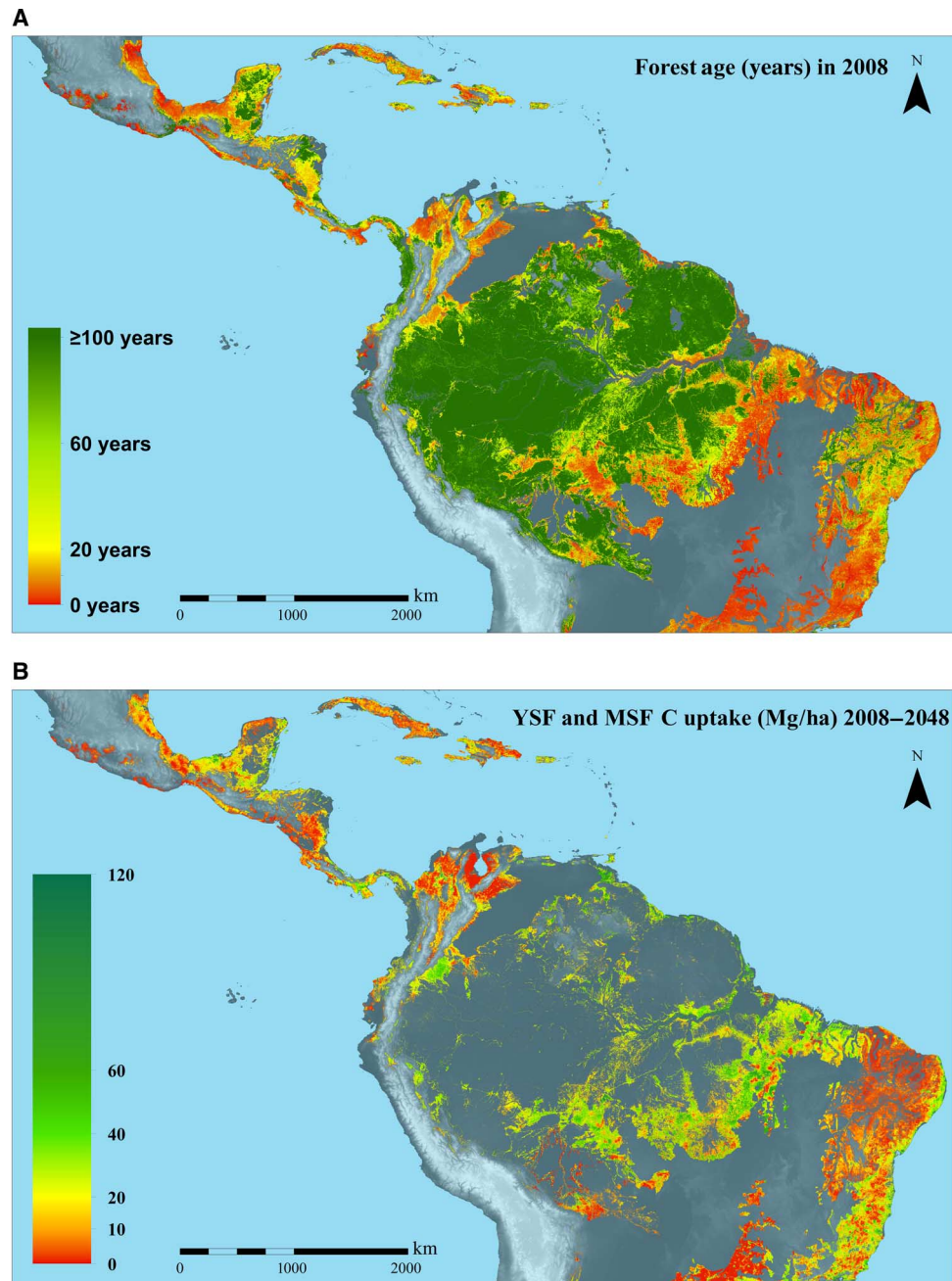


Fig. 2. Age and carbon sequestration maps of a lowland Neotropical forest. (A and B) Modeled mean forest age in 2008 (A), and the total potential sequestered carbon in OGFs, 2008–2048 for all YSFs (≤ 20 years) and MSFs (20 to 60 years) in 2008 (B). The gray areas are areas with no data: above 1000-m altitude, savannas, rivers, lakes, OGFs, or urban areas. The biomes covered are moist and dry tropical forests.

sparing other lands for restoration and forest regeneration (Fig. 3) (35). Natural regeneration on agricultural land must comply with country- and region-specific agendas for maintaining livelihoods and food security and development of sustainable agricultural land use, including agroforestry. Regenerating forests can complement protection of existing OGFs by extending buffer zones and increasing connectivity of forest habitats.

The enormous potential of SFs has been poorly appreciated, despite their growing extent in tropical landscapes (1). In addition to their dual role in both climate change adaptation and mitigation (36, 37), regenerating tropical forests play an important role in biodiversity conservation, increasing connectivity in fragmented landscapes, hydrological regulation, nutrient cycling, and the provision of timber, food, fuel, and fodder to local people (6, 37). The potential carbon sequestration capacity of natural regeneration of YSFs provides a significant low-cost opportunity for carbon sequestration in the tropics while simultaneously benefiting biodiversity and production of multiple ecosystem services, and should be incorporated explicitly into national and international carbon mitigation commitments.

MATERIALS AND METHODS

Experimental design

The study area was located within three major lowland forest biomes (38); 83.2% of forest is in the moist broadleaf biome, whereas 16.8%

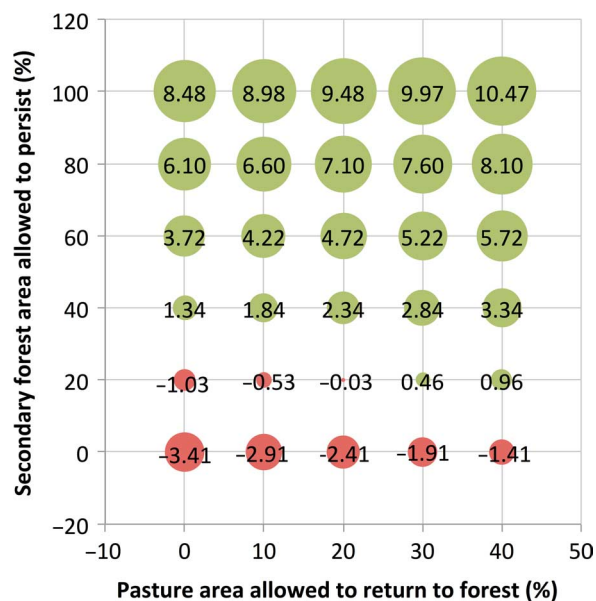


Fig. 3. Potential AGC sequestration (in petagrams) for scenarios of combinations of land use over four decades (2008–2048). Land-use change combinations incorporate the percentage area of land allowed to regenerate following pasture abandonment (0 to 40% cessation of pasture use) and the percentage of YSF (≤ 20 years) and MSF (20 to 60 years) areas allowed to persist and continue regeneration (0 to 100% forest persistence). The size of the circles indicates the potential amount of carbon sequestered. Values in the cells indicate the magnitude of net carbon sequestered over 40 years (in petagrams), with all possible combinations of the two factors. These scenarios account for carbon loss due to SF clearing, which can lead to negative net carbon sequestration (red circles).

is in dry broadleaf and caatinga biomes combined, with each of these biomes having different percentages of secondary forest (see table S1). Across these forest biomes, we estimated the carbon sequestration potential of regrowing forests. Our analysis focused on carbon stored in AGB. We did not estimate biomass stored in soils, belowground biomass, or dead woody debris owing to major uncertainties in these components across biomes, climate zones, and successional stages.

Our approach involved three steps and was based on the most recent and detailed map of Neotropical forest biomass and the largest data set on successional chronosequences compiled to date, including 1148 second-growth plots established in 43 forest sites across the Neotropics (14). In the first step, we estimated the areal extent of existing cleared areas and SFs ≤ 100 years old with potential to regrow. To do so, we used a map of Neotropical forest AGB in 2008 (15) and inferred the ages of these forests, using an equation relating biomass to forest age, and used a map of agricultural lands, including pasture areas in 2000 (10-km pixel size) (39) available at www.earthstat.org/data-download and cropland in 2005 (1-km pixel size) (40) available at www.geo-wiki.org, which provided the percentage of land area with pasture or crops, respectively. In the second step, we assumed that all these regrowth and agricultural areas were allowed to regenerate spontaneously (no active restoration) and projected their biomass accumulation for 40 years into the future, using an equation relating forest age to biomass. In the third step, we relaxed the assumption that all of these areas will regenerate and persist over these projected time scales and modeled carbon sequestration scenarios where 80 to 20% of SF areas undergo regeneration over 40 years. We also simulated carbon sequestration via natural regeneration over 40 years in up to 40% of pasture areas. A detailed description of the 43 study sites is provided by Poorter *et al.* (14).

Mapping areas of different forest ages

We modeled mean forest age and cleared forest (agricultural land use) in the Neotropics based on a 500-m-resolution map of forest biomass (15). Our analysis did not incorporate edge effects, such as increased tree mortality or variation in seed rain with distance from forest sources (41). Further, our approach did not distinguish among logged forests, tree plantations, forests degraded from wildfire, or other disturbances, as spatially explicit data for these cover types are not available across our entire study region. Rather, we limited projections in our study to forests having an initial predicted age of 60 years or less, which we divided into young secondary forests (≤ 20 years of age) and mid-successional secondary forests (between 20 and 60 years of age). General statistics were provided for forests up to 100 years of predicted age for the initial year 2008. This threshold likely excludes most selectively logged or high-graded forests, whereas natural forest areas that experienced intensive logging are likely to have a stand biomass similar to YSFs and are assumed to undergo similar biomass recovery processes (6). However, estimates of forest extent and age would only be slightly affected, as plantations currently cover only 4000 km² in Central America, 150,000 km² in South America, and 7000 km² in the Caribbean (42), which is less than 1% of the estimated extent of YSFs (Fig. 1A). To calculate our maps of forest age and AGB from 2008 to 2048, we used the approach described below.

Our study region focused on the Neotropics, between 23.39°N and -23.41°S [that is, the extent of the pantropical AGB map provided by Baccini *et al.* (15)], and on lowland areas below an altitude of 1000 m based on the distribution of our chronosequence sites (14), as defined by the GTOPO30 digital elevation model available for download at

<https://lta.cr.usgs.gov/GTOPO30>, corresponding to the geographic limits of the locations of our 43 study areas. To distinguish the different forest types, we used a map of world ecoregions (based on potential natural vegetation) obtained from The Nature Conservancy (38) and selected the three principal biomes in which our 43 study sites were located: (i) tropical and subtropical moist broadleaf forests (henceforth referred to as moist forest), (ii) tropical and subtropical dry broadleaf forests, and (iii) caatinga [henceforth (ii) and (iii) are combined and referred to as dry forest]. We then masked all open water bodies, including oceans, lakes, and rivers, using datamask images from Hansen *et al.* (7), which were acquired at a resolution of 30 m × 30 m and which were used to calculate the percentage land cover within each of the 500 m × 500 m study pixels. Urban areas were masked using high-resolution urban maps (43, 44); see Potere *et al.* (45) for a discussion on accuracy assessment. Wetlands were masked using a modified version of the Global Lakes and Wetlands Database created by Lehner and Döll (46), available at <http://www.worldwildlife.org/pages/global-lakes-and-wetlands-database>, which we refined through removal of areas having agriculture or OGF.

The final study area was calculated as the hectares of each pixel occupying terrestrial land surface following adjustment for latitudinal variation in pixel areal extent, which varied from approximately 23.27 ha per pixel at the equator to 21.41 ha per pixel at the northern or southern limit of our study region. All pixels were masked if any portion of the pixel intersected an urban area. We overlaid this map with the map of cropland and pasturelands described above. Here, we refer to both land uses as farmlands.

Estimating 2008 AGB

To obtain AGB (in megagrams per hectare) for each pixel in our study region, we used the Baccini *et al.* (15) map for the year 2008, provided by the Woods Hole Research Center (WHRC), which is the most recently updated highest spatial resolution map of AGB currently available in our study region. AGB (in megagrams per hectare) was obtained at a pixel size of ~500 m × 500 m (25 ha). We inferred forest age from forest biomass and local climatic conditions on the basis of a Michaelis-Menten (MM) equation that relates biomass to mean forest age within the pixel and climatic conditions. The MM equation contains an asymptote parameter a that defines the AGB of OGFs and the parameter a_{50} that defines the age at which 50% of old-growth AGB is reached

$$\text{AGB} = (a \times \text{Age}) / (a_{50} + \text{Age}) \quad (1)$$

We used two different data sets to estimate the parameter values for a and a_{50} . The WHRC map has extensive and continuous climatic and old-growth coverage across the Neotropics, and pixels in national parks were used to estimate the climatic dependence of the old-growth asymptote parameter a , which indicates the maximum AGB. By focusing on national parks only, we minimized reductions in AGB caused by anthropogenic disturbances. The database on secondary forest plots [1148 plots established in 43 chronosequences across the major environmental gradients in the Neotropics (14)] was used to estimate the climatic dependence of parameter a_{50} that determines the shape of the curve, which is mostly determined by young secondary forests. The WHRC map uses, among others, the allometric equation of Chave *et al.* (47) to calculate tree biomass on the basis of stem diameter and wood density. For this reason, we also used the same equation to calculate the biomass for the secondary forest plots of Poorter *et al.* (14), versus the

updated Chave *et al.* 2014 equation (48); this approach ensures consistency with previous carbon estimates across our study area.

We estimated the climate dependence of a (for example, old-growth asymptote) and a_{50} (for example, age at which 50% old-growth asymptote is reached) separately, using a statistical approach to select the most parsimonious subset of four bioclimatic variables from (i) all 19 bioclimatic variables described at www.worldclim.org/bioclim, which were obtained at a 30-s resolution (approximately 1 km × 1 km) from WorldClim (49) (www.worldclim.org/current), and (ii) climatic water deficit (CWD; in millimeters per year), which was obtained from http://chave.ups-tlse.fr/pantropical_allometry.htm. CWD is the amount of water lost during dry months (defined as months where evapotranspiration exceeds rainfall) and is calculated as the total rainfall minus evapotranspiration during dry months. This number is, by definition, negative, and sites with CWD of 0 are not seasonally water stressed. We also used (iii) total soil cation exchange capacity (CEC; in centimoles of positive charge per kilogram of soil), which was used as an indicator of soil fertility. CEC was obtained from the Harmonized World Soil Database from <http://webarchive.iiasa.ac.at/Research/LUC/External-World-soil-database/HTML/>.

To model the climatic dependence of old-growth asymptote a , we developed a geographic (for example, biome) weighted regression approach, which enabled consideration of spatial variation in AGB not accounted for in our selected predictor variables. We made a random selection of 1,639,712 pixels that occurred in less-disturbed areas (that is, parks), had 100% land cover, and were within our biome and elevation (<1000-m altitude) criteria. For this analysis, we used the national parks from the World Database on Protected Areas (WDPA) downloaded in July 2015 from www.protectedplanet.net, and pixels that intersected with protected areas with effective protection from data provided by WDPA were selected. As such, we likely selected pixels that had the maximum old-growth biomass given the climatic conditions. Because of the difference in total area of our study biomes and to avoid having the climatic dependence of a being driven disproportionately by one biome, we randomly selected 10% of identified pixels within moist forest areas ($n = 1,142,833$) and included all identified pixels in dry forest ($n = 349,082$) and caatinga ($n = 147,797$) biomes. We first used a forward stepwise regression of AGB on biome and all bioclimatic variables to identify a parsimonious subset of significant predictor variables, which were mean annual rainfall (in millimeters per year), CWD, soil CEC, and temperature seasonality (expressed as the SD * 100, and defined as variable “BIO4” in WorldClim).

To identify fully intact old-growth pixels, which required excluding pixels with mixed land cover or with low AGB due to other limiting factors (for example, flooding and fire), we ran each model two times, removing pixels identified as outliers (for example, negative residuals ≥ 0.5 STD) during the first run. The final models for moist, dry, and caatinga old-growth AGB were highly significant ($r^2 = 0.39$, $n = 874,222$; $r^2 = 0.66$, $n = 239,764$; and $r^2 = 0.55$, $n = 101,050$, respectively) and highlighted the different controls over AGB in these regions, with moist forest AGB being predicted primarily by CWD and BIO4, dry forest AGB being predicted primarily by CWD and CEC, and caatinga AGB being predicted by CWD and mean annual precipitation. To validate the final map of old-growth AGB, we used an independent group of randomly selected points widely distributed across all biomes within our study region

that we manually verified through recent (year 2013+) high-resolution (<5 m × 5 m pixels) satellite imagery to be representative of intact forest at that location, and ran a linear regression between our predicted AGB values at that location and those extracted from the WHRC AGB map. This validation found our old-growth AGB prediction model to be highly significant ($r^2 = 0.70$, $n = 500$). The final model and coefficients for moist, dry, and caatinga are as follows

$$a \text{ (Moist)} = 370 - 0.0133 * \text{Precipitation} + 0.1586 * \text{CWD} - 0.1235 * \text{CEC} - 0.0191 * \text{BIO4} \quad (2)$$

$$a \text{ (Dry)} = 330 + 0.0053 * \text{Precipitation} + 0.1984 * \text{CWD} - 1.6974 * \text{CEC} - 0.0084 * \text{BIO4} \quad (3)$$

$$a \text{ (Caatinga)} = 158 + 0.0398 * \text{Precipitation} + 0.0941 * \text{CWD} - 0.8300 * \text{CEC} - 0.0018 * \text{BIO4} \quad (4)$$

To model the climatic dependence of a_{50} , we included the effects of mean annual precipitation, rainfall seasonality (expressed as a coefficient of variation, and defined as variable “BIO15” in WorldClim), and CWD (14). We then used nonlinear regression to fit Eq. 1 to the secondary forest data, using Eqs. 2 to 4 for asymptote a , depending on their biome

$$a_{50} = 26.4368 - 0.004927 \times \text{CWD} + 0.001321 \times \text{Rainfall} - 0.290429 \times \text{Rainfall seasonality} \quad (5)$$

We then inverted Eq. 1 to estimate for each pixel its age from AGB

$$\text{Age} = (a_{50} \times \text{AGB}) / (a - \text{AGB}) \quad (6)$$

where age is in years and AGB is the pixel AGB provided by WHRC 2008. We used Eq. 6 to make an age map of Neotropical forests. Some age estimates were greater than 300 years, because the observed AGB pixel values were close to, or exceeded, those of predicted old-growth values. For those pixels, the age was set to 300 years and AGB values were set to the pixel AGB provided by WHRC 2008. It is important to note that age estimates pertain to the mean value of each pixel, as we cannot resolve forest ages at subpixel resolution. The biomass map we used is, nevertheless, the highest-resolution map currently available, and therefore provides the best estimate. With the arrival of higher-resolution 30 m × 30 m land-use and biomass maps, the accuracy of our predictions may be further improved.

Uncertainty analysis

We performed an uncertainty analysis by calculating the bootstrapped SDs of all parameter estimates and then used a Monte Carlo procedure with 10,000 uniformly random selected parameter combinations within 1 SD of all mean parameter estimates for each pixel in our study region. We then calculated the mean and SD of the predicted age of each combination for each pixel. The mean value was used to create our final map of forest age in 2008, and we calculated the total uncertainty by

calculating the total AGB in young secondary forests (≤ 20 years of age) and mid-secondary forests (between 20 and 60 years of age) as projected, as well as at the lower and upper SD value, and summed these across pixels to provide a measure of uncertainty associated with the total carbon sequestration potential of SFs. The pixel size of our final AGB map is 500 m × 500 m, and we acknowledge that our pixel mean age in many cases will be composed of different aged forests and, in some cases, a mixture of land cover types, such as pasture, secondary forest, and OGF. Although we did not incorporate uncertainty related to mixed pixel land covers across our entire study region, we did conduct tests using hypothetical mixtures of land cover types for selected pixels, and our results showed that variation in carbon gain from 2008 to 2048 resulting from different proportions of forest age was less than the uncertainty resulting from the per-pixel forest age estimation, calculated as the Monte Carlo mean and SD of each pixel's predicted forest age. At the local or regional scale, however, such within-pixel variations can be considerable and may result in deviations from the overall pattern.

For most analyses, forest age was grouped into four classes: YSF (≤ 20 years), MSF (between 20 and 60 years), old SF (between 60 and 100 years), and OGF (> 100 years). We set the threshold age for OGFs arbitrarily at 100 years, because we did not have data for older second-growth plots. After 100 years, the forest is well developed in terms of species richness, structure, and biomass, although species composition and soil characteristics may take much longer to recover.

Projecting AGB accumulation in SFs

For subsequent analyses related to our AGB projections, we focused on young (1 to 20 years) and intermediate (20 to 60 years) second-growth pixels identified in 2008. For each pixel, we predicted the AGB accumulation over 40 years, from 2008 to 2048. We focused on 40 years, because calculating AGB in forests older than 100 years (that is, 60 years plus the projected 40 years) would be extrapolating beyond the maximum SF age of the chronosequences we used to develop the equations (15). To calculate AGB from age for our future age distribution maps, we used Eq. 1.

We used the projected biomass accumulation to biomass stocks and sequestration for moist and dry forest types, countries (tables S1 and S2, respectively), and years (see Fig. 1D for increase in carbon stock in young plus mid-age secondary forests for the whole Latin American study region and Fig. 1E for increase in carbon stock in young plus mid-age secondary forests in the four countries with the largest increase over the four decades). To calculate mean annual carbon sequestration rates, we used net AGB change, multiplied it by 0.5 [which is the average carbon value in dry biomass and widely used in the literature, such as by Baccini *et al.* (15) on which our initial AGB estimates are based], and divided it over the time interval considered. Because annual rates of AGC storage vary greatly with secondary forest age, we provided mean annual sequestration rates separately for YSF for 2008 and MSF for the periods 2008–2013 and 2043–2048.

Analysis of natural regeneration scenarios

Natural regeneration will not always occur at its full potential because of ecological, geographical, and socioeconomic constraints. To evaluate the effects of reduced secondary regrowth to carbon mitigation (Fig. 1C), we used six scenarios in which the available area allowed to follow natural regeneration was set to 100, 80, 60, 40, 20, or 0%, and assumed

no spatial variation in rates of biomass recovery beyond the effects of climate. The carbon stock in the nonselected pixels (secondary forest pixels that were supposed to be transformed into agricultural land) was set to the average carbon stock found in agricultural land pixels, which was calculated as the area-weighted average of crop land pixels and pasture land pixels ($49.9 \text{ Mg C ha}^{-1}$).

To evaluate the effects on carbon sequestration of a combination of scenarios of reduced secondary regrowth and reduced regrowth of agricultural land (Fig. 3), we combined six scenarios of secondary forest regeneration, both YSF and MSF (100, 80, 60, 40, 20, or 0%), with five scenarios of areas of forest regeneration on pasture land (40, 30, 20, 10, or 0%), which we considered realistic on the basis of recent data of forest regrowth on abandoned pastures in Para, Brazil (50). These scenarios can also simulate cases where natural regeneration is compromised by former land use or lack of seed dispersal (6). We applied these filters as described above to create Fig. 1C. The carbon stock in recovering pasture pixels recovers following the modeled calculations described for those pixels. The carbon stock in the nonselected agricultural land pixels remained as the carbon stock that they had in 2008.

All analyses related to the development of the age-to-AGB relationship were performed in R 3.1.2, and all analyses related to the spatial and temporal modeling and mapping were performed in the Interactive Data Language (version 8.2).

SUPPLEMENTARY MATERIALS

Supplementary material for this article is available at <http://advances.sciencemag.org/cgi/content/full/2/5/e1501639/DC1>

fig. S1. Carbon sequestration potential during 2008–2048 for crop areas of a lowland Neotropical forest.

fig. S2. Carbon sequestration potential during 2008–2048 for pasture areas of a lowland Neotropical forest.

fig. S3. Carbon sequestration potential during 2008–2048 for areas of YSFs and MSFs (in 2008), crops, and pasture combined.

table S1. Area, carbon stocks, and sequestration potential of different land cover types in lowland moist and dry tropical forest biomes.

table S2. Area, carbon stocks, and sequestration potential of Latin American countries.

table S3. Ranked area, carbon stocks, and sequestration potential of different land cover types in lowland moist and dry tropical forest biomes of the top 10 Latin American countries.

REFERENCES AND NOTES

- R. A. Houghton, B. Byers, A. A. Nassikas, A role for tropical forests in stabilizing atmospheric CO_2 . *Nat. Clim. Chang.* **5**, 1022–1023 (2015).
- Y. Pan, R. A. Birdsey, J. Fang, R. Houghton, P. E. Kauppi, W. A. Kurz, O. L. Phillips, A. Shvidenko, S. L. Lewis, J. G. Canadell, P. Ciais, R. B. Jackson, S. W. Pacala, A. D. McGuire, S. Piao, A. Rautiainen, S. Sitch, D. Hayes, A large and persistent carbon sink in the world's forests. *Science* **333**, 988–993 (2011).
- S. J. Wright, The carbon sink in intact tropical forests. *Glob. Chang. Biol.* **19**, 337–339 (2013).
- FAO, *Global Forest Resources Assessment 2015. How Are the World's Forests Changing?* (FAO, Rome, Italy, 2015).
- T. M. Aide, M. L. Clark, H. R. Grau, D. López-Carr, M. A. Levy, D. Redo, M. Bonilla-Moheno, G. Riner, M. J. Andrade-Núñez, M. Muñiz, Deforestation and reforestation of Latin America and the Caribbean (2001–2010). *Biotropica* **45**, 262–271 (2013).
- R. L. Chazdon, *Second Growth: The Promise of Tropical Forest Regeneration in an Age of Deforestation* (University of Chicago Press, Chicago, IL, 2014), 485 pp.
- M. C. Hansen, P. V. Potapov, R. Moore, M. Hancher, S. A. Turubanova, A. Tyukavina, D. Thau, S. V. Stehman, S. J. Goetz, T. R. Loveland, A. Kommareddy, A. Egorov, L. Chini, C. O. Justice, J. R. G. Townshend, High-resolution global maps of 21st-century forest cover change. *Science* **342**, 850–853 (2013).
- J. G. Canadell, M. R. Raupach, Managing forests for climate change mitigation. *Science* **320**, 1456–1457 (2008).
- R. A. Houghton, in *Global Forest Monitoring from Earth Observation*, F. Achard, M. C. Hansen, Eds. (CRC Press, Boca Raton, FL, 2013), pp. 15–38.
- R. C. Goodman, M. Herold, Why maintaining tropical forests is essential and urgent for a stable climate, in *CGD Climate and Forest Paper Series #11* (Center for Global Development Climate and Forest, Washington, DC, 2014), 56 pp.
- M. van Breugel, J. S. Hall, D. Craven, M. Bailon, A. Hernandez, M. Abbene, P. van Breugel, Succession of ephemeral secondary forests and their limited role for the conservation of floristic diversity in a human-modified tropical landscape. *PLOS One* **8**, e82433 (2013).
- A. P. D. Aguiar, I. C. G. Vieira, T. O. Assis, E. L. Dalla-Nora, P. M. Toledo, R. A. Oliveira Santos-Junior, M. Batistella, A. S. Coelho, E. K. Savaget, L. E. O. C. Aragão, C. A. Nobre, J. P. H. Ometto, Land use change emission scenarios: Anticipating a forest transition process in the Brazilian Amazon. *Glob. Chang. Biol.* **22**, 1821–1840 (2016).
- M. K. Steininger, Net carbon fluxes from forest clearance and regrowth in the Amazon. *Ecol. Appl.* **14**, S313–S322 (2004).
- L. Poorter, F. Bongers, T. M. Aide, A. M. Almeyda Zambrano, P. Balvanera, J. M. Becknell, V. Boukili, P. H. S. Brancalion, E. N. Broadbent, R. L. Chazdon, D. Craven, J. S. de Almeida-Cortez, G. A. L. Cabral, B. H. J. de Jong, J. S. Denslow, D. H. Dent, S. J. DeWalt, J. M. Dupuy, S. M. Durán, M. M. Espírito-Santo, M. C. Fandino, R. G. César, J. S. Hall, J. L. Hernandez-Stefanoni, C. C. Jakovac, A. B. Junqueira, D. Kennard, S. G. Letcher, J.-C. Licona, M. Lohbeck, E. Marin-Spiotta, M. Martínez-Ramos, P. Massoca, J. A. Meave, R. Mesquita, F. Mora, R. Muñoz, R. Muscarella, Y. R. F. Nunes, S. Ochoa-Gaona, A. A. de Oliveira, E. Orihuela-Belmonte, M. Peña-Claros, E. A. Pérez-García, D. Píotto, J. S. Powers, J. Rodríguez-Velázquez, I. E. Romero-Pérez, J. Ruíz, J. G. Saldarriaga, A. Sanchez-Azofeifa, N. B. Schwartz, M. K. Steininger, N. G. Swenson, M. Toledo, M. Uriarte, M. van Breugel, H. van der Wal, M. D. M. Veloso, H. F. M. Vester, A. Vicentini, I. C. G. Vieira, T. V. Bentsos, G. B. Williamson, D. M. A. Rozendaal, Biomass resilience of Neotropical secondary forests. *Nature* **530**, 211–214 (2016).
- A. Baccini, S. J. Goetz, W. S. Walker, N. T. Laporte, M. Sun, D. Sulla-Menashe, J. Hackler, P. S. A. Beck, R. Dubayah, M. A. Friedl, S. Samanta, R. A. Houghton, Estimated carbon dioxide emissions from tropical deforestation improved by carbon-density maps. *Nat. Clim. Chang.* **2**, 182–185 (2012).
- B. B. N. Strassburg, A. E. Latawiec, L. G. Barioni, C. A. Nobre, V. P. da Silva, J. F. Valentim, M. Vianna, E. D. Assad, When enough should be enough: Improving the use of current agricultural lands could meet production demands and spare natural habitats in Brazil. *Glob. Environ. Chang.* **28**, 84–97 (2014).
- B. Soares-Filho, R. Rajão, M. Macedo, A. Carneiro, W. Costa, M. Coe, H. Rodrigues, A. Alencar, Cracking Brazil's Forest Code. *Science* **344**, 363–364 (2014).
- J. G. J. Olivier, G. Janssens-Maenhout, M. Muntean, J. A. H. W. Petes, *Trends in Global CO_2 Emissions: 2015 Report*, PBL Netherlands Environmental Assessment Agency, The Hague; European Commission, Joint Research Centre (JRC), Institute for Environment and Sustainability (IES). JRC98184, PBL1803; http://edgar.jrc.ec.europa.eu/news_docs/jrc-2015-trends-in-global-co2-emissions-2015-report-98184.pdf [accessed November 2015].
- IPCC, "Annex II: Glossary [Mach, K. J., S. Planton and C. von Stechow (Eds.)], *Climate Change 2014: Synthesis Report. Contribution of Working Groups I, II and III to the Fifth Assessment Report of the Intergovernmental Panel on Climate Change* (IPCC, Geneva, Switzerland, 2014), 151 pp.
- I. C. G. Vieira, T. Gardner, J. Ferreira, A. C. Lees, J. Barlow, Challenges of governing second-growth forests: A case study from the Brazilian Amazonian State of Pará. *Forests* **5**, 1737–1752 (2014).
- FAO, *Global Forest Resources Assessment 2010* (Food and Agricultural Organization of the United Nations, Rome, Italy, 2010), 378 pp.
- J. A. Gallardo-Cruz, J. A. Meave, E. J. González, E. E. Lebrija-Trejos, M. A. Romero-Romero, E. A. Pérez-García, R. Gallardo-Cruz, J. L. Hernández-Stefanoni, C. Martorell, Predicting tropical dry forest successional attributes from space: Is the key hidden in image texture? *PLOS One* **7**, e30506 (2012).
- M. E. Fagan, R. S. DeFries, S. E. Slesnie, J. P. Arroyo-Mora, C. Soto, A. Singh, P. A. Townsend, R. L. Chazdon, Mapping species composition of forests and tree plantations in Northeastern Costa Rica with an integration of hyperspectral and multitemporal Landsat imagery. *Remote Sens.* **7**, 5660–5696 (2015).
- R. Petersen, E. D. Goldman, N. Harris, S. Sargent, D. Aksenov, A. Manisha, E. Espipova, V. Shevade, T. Loboda, N. Kuksina, I. Kurakina, *Mapping Tree Plantations with Multispectral Imagery: Preliminary Results for Seven Tropical Countries* (World Resources Institute, Washington, DC); www.wri.org/publication/mapping-treeplantations.
- S. Luyssaert, I. Inglima, M. Jung, A. D. Richardson, M. Reichstein, D. Papale, S. L. Piao, E.-D. Schulze, L. Wingate, G. Matteucci, L. Aragao, M. Aubinet, C. Beer, C. Bernhofer, K. G. Black, D. Bonal, J.-M. Bonnefond, J. Chambers, P. Ciais, B. Cook, K. J. Davis, A. J. Dolman, B. Gielen, M. Goulden, J. Grace, A. Granier, A. Grelle, T. Griffis, T. Grünwald, G. Guidolotti, P. J. Hanson, R. Harding, D. Y. Hollinger, L. R. Hutrya, P. Kolari, B. Kruijt, W. Kutsch, F. Lagergren, T. Laurila, B. E. Law, G. Le Maire, A. Lindroth, D. Loustau, Y. Malhi, J. Mateus, M. Migliavacca, L. Misson, L. Montagnani, J. Moncrieff, E. Moors, J. W. Munger, E. Nikinmaa, S. V. Ollinger, G. Pita, C. Rebmann, O. Roupsard, N. Saigusa, M. J. Sanz, G. Seufert, C. Sierra, M.-L. Smith, J. Tang, R. Valentini, T. Vesala, I. A. Janssens, CO_2 balance of boreal, temperate, and tropical forests derived from a global database. *Glob. Chang. Biol.* **13**, 2509–2537 (2007).

26. J. S. Powers, M. D. Corre, T. E. Twine, E. Veldkamp, Geographic bias of field observations of soil carbon stocks with tropical land-use changes precludes spatial extrapolation. *Proc. Natl. Acad. Sci. U.S.A.* **108**, 6318–6322 (2011).
27. A. K. Skidmore, N. Pettorelli, N. C. Coops, G. N. Geller, M. Hansen, R. Lucas, C. A. Múcher, B. O'Connor, M. Paganini, H. M. Pereira, M. E. Schaepman, W. Turner, T. Wang, M. Wegmann, Environmental science: Agree on biodiversity metrics to track from space. *Nature* **523**, 403–405 (2015).
28. E. Marin-Spiotta, D. F. Cusack, R. Ostertag, W. L. Silver, in *Post-Agricultural Succession in the Neotropics*, R. W. Myster, Ed. (Springer, New York, 2008), pp. 22–72.
29. E. V. Wandelli, P. M. Fearnside, Secondary vegetation in central Amazonia: Land-use history effects on aboveground biomass. *For. Ecol. Manage.* **347**, 140–148 (2015).
30. S. A. Mukul, J. Herbohn, J. Firn, Tropical secondary forests regenerating after shifting cultivation in the Philippines uplands are important carbon sinks. *Sci. Rep.* **6**, 22483 (2016).
31. K. J. Anderson-Teixeira, M. M. H. Wang, J. C. McGarvey, D. S. LeBauer, Carbon dynamics of mature and regrowth tropical forests derived from a pantropical database (TropForC-db). *Glob. Chang. Biol.* **22**, 1690–1709 (2016).
32. M. Greve, B. Beyers, A. M. Lykke, J.-C. Svenning, Spatial optimization of carbon-stocking projects across Africa integrating stocking potential with co-benefits and feasibility. *Nat. Commun.* **4**, 2975 (2013).
33. M. Uriarte, J. R. Lasky, V. K. Boukili, R. L. Chazdon, A trait-mediated, neighbourhood approach to quantify climate impacts on successional dynamics of tropical rainforests. *Funct. Ecol.* **30**, 157–167 (2016).
34. Federal Republic of Brazil, <http://www4.unfccc.int/submissions/INDC/Published%20Documents/Brazil/1/BRAZIL%20INDC%20english%20FINAL.pdf> [accessed October 28, 2015].
35. A. E. Latawiec, B. B. N. Strassburg, P. H. S. Brancalion, R. R. Rodrigues, T. Gardner, Creating space for large-scale restoration in tropical agricultural landscapes. *Front. Ecol. Environ.* **13**, 211–218 (2015).
36. B. Locatelli, C. P. Catterall, P. Imbach, C. Kumar, R. Lasco, E. Marin-Spiotta, B. Mercer, J. S. Powers, N. Schwartz, M. Uriarte, Tropical reforestation and climate change: Beyond carbon. *Restor. Ecol.* **23**, 337–343 (2015).
37. J. A. Stanturf, P. Kant, J.-P. B. Lillesø, S. Mansourian, M. Kleine, L. Graudal, P. Madsen, *Forest Landscape Restoration as a Key Component of Climate Change Mitigation and Adaptation* (IUFRO World Series, Vienna, Austria, 2015), vol. 34, 72 pp.
38. D. M. Olson, E. Dinerstein, E. D. Wikramanayake, N. D. Burgess, G. V. N. Powell, E. C. Underwood, J. A. D'Amico, I. Itoua, H. E. Strand, J. C. Morrison, C. J. Loucks, T. F. Allnutt, T. H. Ricketts, Y. Kura, J. F. Lamoreux, W. W. Wettengel, P. Hedao, K. R. Kassem, Terrestrial ecoregions of the world: A new map of life on Earth. *Bioscience* **51**, 933–938 (2001).
39. N. Ramankutty, A. T. Evan, C. Monfreda, J. A. Foley, Farming the planet: 1. Geographic distribution of global agricultural lands in the year 2000. *Global Biogeochem. Cycles* **22**, GB1003 (2008).
40. S. Fritz, L. See, I. McCallum, L. You, A. Bun, E. Moltchanova, M. Duerauer, F. Albrecht, C. Schill, C. Perger, P. Havlik, A. Mosnier, P. Thornton, U. Wood-Sichra, M. Herrero, I. Becker-Reshef, C. Justice, M. Hansen, P. Gong, S. Abdel Aziz, A. Cipriani, R. Cumani, G. Cecchi, G. Conchedda, S. Ferreira, A. Gomez, M. Haffani, F. Kayitani, J. Malanding, R. Mueller, T. Newby, A. Nonguierma, A. Olusegun, S. Ortner, D. R. Rajak, J. Rocha, D. Schepaschenko, M. Schepaschenko, A. Terekhov, A. Tiangwa, C. Vancutsem, E. Vintrou, W. Wenbin, M. van der Velde, A. Dunwoody, F. Kraxner, M. Obersteiner, Mapping global cropland and field size. *Glob. Chang. Biol.* **21**, 1980–1992 (2015).
41. R. Chaplin-Kramer, I. Ramler, R. Sharp, N. M. Haddad, J. S. Gerber, P. C. West, L. Mandler, P. Engstrom, A. Baccini, S. Sim, C. Mueller, H. King, Degradation in carbon stocks near tropical forest edges. *Nat. Commun.* **6**, 10158 (2015).
42. T. Payn, J.-M. Carnus, P. Freer-Smith, M. Kimberley, W. Kollert, S. Liu, C. Orazio, L. Rodriguez, L. N. Silva, M. J. Wingfield, Changes in planted forests and future global implications. *For. Ecol. Manage.* **352**, 57–67 (2015).
43. A. Schneider, M. A. Friedl, D. Potere, A new map of global urban extent from MODIS satellite data. *Environ. Res. Lett.* **4**, 044003 (2009).
44. A. Schneider, M. A. Friedl, D. Potere, Mapping global urban areas using MODIS 500-m data: New methods and datasets based on 'urban ecoregions'. *Remote Sens. Environ.* **114**, 1733–1746 (2010).
45. D. Potere, A. Schneider, S. Angel, D. L. Civco, Mapping urban areas on a global scale: Which of the eight maps now available is more accurate? *Int. J. Remote Sens.* **30**, 6531–6558 (2009).
46. B. Lehner, P. Döll, Development and validation of a global database of lakes, reservoirs and wetlands. *J. Hydrol.* **296**, 1–22 (2004).
47. J. Chave, C. Andalo, S. Brown, M. A. Cairns, J. Q. Chambers, D. Eamus, H. Fölster, F. Fromard, N. Higuchi, T. Kira, J.-P. Lescuré, B. W. Nelson, H. Ogawa, H. Puig, B. Riéra, T. Yamakura, Tree allometry and improved estimation of carbon stocks and balance in tropical forests. *Oecologia* **145**, 87–99 (2005).
48. J. Chave, M. Réjou-Méchain, A. Búrquez, E. Chidumayo, M. S. Colgan, W. B. C. Delitti, A. Duque, T. Eid, P. M. Fearnside, R. C. Goodman, M. Henry, A. Martínez-Yrizar, W. A. Mugasha, H. C. Muller-Landau, M. Mencuccini, B. W. Nelson, A. Ngomanda, E. M. Nogueira, E. Ortiz-Malavassi, R. Péliissier, P. Ploton, C. M. Ryan, J. G. Saldarriaga, G. Vieilledent, Improved allometric models to estimate the aboveground biomass of tropical trees. *Glob. Chang. Biol.* **20**, 3177–3190 (2014).
49. R. J. Hijmans, S. E. Cameron, J. L. Parra, P. G. Jones, A. Jarvis, Very high resolution interpolated climate surfaces for global land areas. *Int. J. Climatol.* **25**, 1965–1978 (2005).
50. EMBRAPA-INPE, Levantamento de informacoes de use e cobertura da terra na Amazonia. *Sumario Executivo* (2011).

Acknowledgments: This paper is a product of the 2ndFOR collaborative research network on secondary forests. We thank the owners of the secondary forest sites for access to their forests, all the people who have established and measured the plots, and the institutions and funding agencies that supported them. We thank E. Marin-Spiotta, M. Toledo, and J. Zimmerman for the use of plot data. E. Arets provided assistance with carbon mitigation calculations. N. Pitman provided constructive comments on an earlier version of this manuscript. This is publication #685 in the Technical Series of the Biological Dynamics of Forest Fragments Project BDFPP-INPA-SI.

Funding: The following agencies provided financial support for this research: the Australian Department of Foreign Affairs and Trade, Consultative Group for International Agricultural Research (CGIAR) Forests, Trees, and Agroforestry (FTA) Program, the Center for International Forestry Research, Colciencias grant 1243-13-16640, Consejo Nacional de Ciencia y Tecnología (SEP-CONACYT 2009-129740 and SEP-CONACYT 2015-255544 for ReSeRbos, CONACYT 33851-B, SEMARNAT-CONACYT 2002 C01-0597, SEP-CONACYT CB-2005-01-51043, and PAPIIT-DGAPA IN213714 and IND211114), PAPIIT-UNAM (IN221503-3), CONACYT (CB-2009-01-128136), Conselho Nacional de Desenvolvimento Científico e Tecnológico (CNPq 563304/2010-3, 562955/2010-0, and PQ 307422/2012-7), Instituto Tamandua, FOMIX-Yucatan (YUC-2008-C06-108863), ForestGEO, Fundação de Amparo à Pesquisa de Minas Gerais (FAPEMIG CRA APQ-0001-11), Fundação Ecológica de Cuixmal, the Heising-Simons Foundation, HSBC, ICETEX, Instituto Internacional de Educação do Brasil, Instituto Nacional de Serviços Ambientais da Amazônia-Instituto Nacional de Pesquisas da Amazônia, the Inter-American Institute for Global Change (Tropi-dry network CRN3-025), the Motta Family Foundation, NSF (NSF-DEB 0639114, 0639393, 1147429, 0129104, 1050957, 1147434, CAREER GRANT DEB-1053237, NSF BCS-1349952, and NSF-CNH-RCN grant 1313788 for Tropical Reforestation Network: Building a Socioecological Understanding of Tropical Reforestation), NUFFIC, USAID (BOLF0R), INCT Biodiversidade e Uso da Terra na Amazônia (CNPq 574008/2008-0), the Silicon Valley Foundation, Stichting Het Kronendak, the Tropenbos Foundation, and Wageningen University (INREF Terra Preta programme and FOREFRONT programme). This study was partly funded by European Union's Seventh Framework Programme (FP7/2007-2013) under grant agreement no. 283093 [Role Of Biodiversity In climate change mitigation (ROBIN)].

Author contributions: R.L.C., E.N.B., D.M.A.R., L.P., F.B., and A.M.A.Z. designed the study and contributed to the manuscript; R.L.C. led the writing and editing of the manuscript; E.N.B., D.M.A.R., and A.M.A.Z. conducted data analysis and produced maps; all authors contributed data and provided comments on the manuscript. **Competing interests:** The authors declare that they have no competing interests. **Data and materials availability:** All data needed to evaluate the conclusions in the paper are present in the paper and/or the Supplementary Materials or are derived from publicly available sources. Additional data related to this paper are available from the authors upon request.

Submitted 13 November 2015

Accepted 12 April 2016

Published 13 May 2016

10.1126/sciadv.1501639

Citation: R. L. Chazdon, E. N. Broadbent, D. M. A. Rozendaal, F. Bongers, A. M. A. Zambrano, T. M. Aide, P. Balvanera, J. M. Becknell, V. Boukili, P. H. S. Brancalion, D. Craven, J. S. Almeida-Cortez, G. A. L. Cabral, B. de Jong, J. S. Denslow, D. H. Dent, S. J. DeWalt, J. M. Dupuy, S. M. Durán, M. M. Espírito-Santo, M. C. Fandino, R. G. César, J. S. Hall, J. L. Hernández-Stefanoni, C. C. Jakovac, A. B. Junqueira, D. Kennard, S. G. Letcher, M. Lohbeck, M. Martínez-Ramos, P. Massoca, J. A. Meave, R. Mesquita, F. Mora, R. Muñoz, R. Muscarella, Y. R. F. Nunes, S. Ochoa-Gaona, E. Orihuela-Belmonte, M. Peña-Claros, E. A. Pérez-García, D. Piotta, J. S. Powers, J. Rodríguez-Velázquez, I. Eunice Romero-Pérez, J. Ruiz, J. G. Saldarriaga, A. Sanchez-Azofeifa, N. B. Schwartz, M. K. Steininger, N. G. Swenson, M. Uriarte, M. van Breugel, H. van der Wal, M. D. M. Veloso, H. Vester, I. C. G. Vieira, T. V. Bentos, G. B. Williamson, L. Poorter, Carbon sequestration potential of second-growth forest regeneration in the Latin American tropics. *Sci. Adv.* **2**, e1501639 (2016).

Carbon sequestration potential of second-growth forest regeneration in the Latin American tropics

Robin L. Chazdon, Eben N. Broadbent, Danaë M. A. Rozendaal, Frans Bongers, Angélica María Almeyda Zambrano, T. Mitchell Aide, Patricia Balvanera, Justin M. Becknell, Vanessa Boukili, Pedro H. S. Brancalion, Dylan Craven, Jarcilene S. Almeida-Cortez, George A. L. Cabral, Ben de Jong, Julie S. Denslow, Daisy H. Dent, Saara J. DeWalt, Juan M. Dupuy, Sandra M. Durán, Mario M. Espírito-Santo, María C. Fandino, Ricardo G. César, Jefferson S. Hall, José Luis Hernández-Stefanoni, Catarina C. Jakovac, André B. Junqueira, Deborah Kennard, Susan G. Letcher, Madelon Lohbeck, Miguel Martínez-Ramos, Paulo Massoca, Jorge A. Meave, Rita Mesquita, Francisco Mora, Rodrigo Muñoz, Robert Muscarella, Yule R. F. Nunes, Susana Ochoa-Gaona, Edith Orihuela-Belmonte, Marielos Peña-Claros, Eduardo A. Pérez-García, Daniel Piotto, Jennifer S. Powers, Jorge Rodríguez-Velazquez, Isabel Eunice Romero-Pérez, Jorge Ruíz, Juan G. Saldarriaga, Arturo Sanchez-Azofeifa, Naomi B. Schwartz, Marc K. Steininger, Nathan G. Swenson, Maria Uriarte, Michiel van Breugel, Hans van der Wal, Maria D. M. Veloso, Hans Vester, Ima Celia G. Vieira, Tony Vizcarra Bentos, G. Bruce Williamson and Lourens Poorter (May 13, 2016)
Sci Adv 2016, 2:
doi: 10.1126/sciadv.1501639

This article is published under a Creative Commons license. The specific license under which this article is published is noted on the first page.

For articles published under [CC BY](#) licenses, you may freely distribute, adapt, or reuse the article, including for commercial purposes, provided you give proper attribution.

For articles published under [CC BY-NC](#) licenses, you may distribute, adapt, or reuse the article for non-commercial purposes. Commercial use requires prior permission from the American Association for the Advancement of Science (AAAS). You may request permission by clicking [here](#).

The following resources related to this article are available online at <http://advances.sciencemag.org>. (This information is current as of May 23, 2017):

Updated information and services, including high-resolution figures, can be found in the online version of this article at:

<http://advances.sciencemag.org/content/2/5/e1501639.full>

Supporting Online Material can be found at:

<http://advances.sciencemag.org/content/suppl/2016/05/10/2.5.e1501639.DC1>

This article **cites 38 articles**, 6 of which you can access for free at:

<http://advances.sciencemag.org/content/2/5/e1501639#BIBL>

Science Advances (ISSN 2375-2548) publishes new articles weekly. The journal is published by the American Association for the Advancement of Science (AAAS), 1200 New York Avenue NW, Washington, DC 20005. Copyright is held by the Authors unless stated otherwise. AAAS is the exclusive licensee. The title *Science Advances* is a registered trademark of AAAS